Conf-751116--7

DESIGN OF OPTIMIZED RC-CR FILTERS FOR CURRENT-PULSE OPERATION OF FISSION COUNTERS AND HIGH SENSITIVITY FISSION COUNTERS FOR HIGH GAMMA BACKGROUNDS*

J. T. DeLorenzo

Oak Ridge National Laboratory
Oak Ridge, Tennessee 37830

ABSTRACT

A calculational procedure was developed to design RC-CR filters for processing current pulses from fission counters in a gamma background ranging from 10^5 to 6×10^6 R/hr. The effects of noise from the gamma background and the input preamplifier and of the time constant of the fission counter and input cable were studied. Analytical results were in close agreement with experimental data. A pole-zero network was examined as a means of compensating for the time constant of the fission counter and input cable, but its improvement was insignificant.

The procedure was expanded to design a high sensitivity, gamma-tolerant fission counter (~10 counts sec^{-1} nv^{-1} at 10^5 R/hr), and the result was a conceptual design with a performance almost equal to a recently developed high temperature fission counter.

*Research sponsored by the Energy Research and Development Administration under contract with the Union Carbide Corporation.

1. INTRODUCTION

Highly efficient detection of neutrons with a fission counter in gamma fields from 10^5 to 6×10^6 R/hr, which will be required for an in-vessel flux monitor in future liquid-metal fast breeder reactors, has stimulated the application of current-pulse processing systems.[1] Usually, RC-CR filters* are a part of such systems to limit the bandwidth to obtain the best noise-to-signal ratio.** There has been no analytical work to optimize such a filter for this application, and it has been only recently that an experimental optimization was made for an ORNL developmental, high temperature fission counter.[2] (This counter is now undergoing life tests in the experimental breeder reactor, EBR-II).

Because ex-vessel neutron detectors are being considered for low-level flux monitors, a detector having a minimum sensitivity of ~10 counts sec^{-1} nv^{-1} might be required. The proved reliability of the fission counter makes it a prime candidate for this application; however, the capacitance created by the large electrode areas required to yield such a high sensitivity would tend to severely reduce the noise-to-signal ratio. The analytical procedure for optimization of the RC-Cr filter was applied to determine whether the design of a high sensitivity fission counter is feasible.

The optimization procedure for the RC-CR filter required the calculation of a noise-to-signal ratio.[3-6] The spectra of the gamma background and preamplifier noise are used to determine the total rms noise transmitted by the filter. The gamma spectrum was obtained

---

* RC-delay line type filters were investigated also, but since preliminary results did not yield any significant improvement, the work was terminated.

** The ratio of "noise-to-signal" in lieu of the more common expression of "signal-to-noise" was chosen to be consistent with recent literature relating to signal and noise for nuclear particle detection.

from spectral measurements with the high temperature fission counter. From an approximation of the current-pulse shape and a normalized amplitude, the peak voltage transmitted by the filter can be computed to complete the determination of the ratio. (This procedure disregards counting resolution, and if it is a factor, some trade-off will be required.) Both the gamma noise and peak voltage are strongly influenced by a time constant that is a function of the counter capacitance and signal cable characteristic impedance. An expression for this time constant in terms of the interelectrode capacitances of a guarded counter is derived and the effect of this time constant on the optimization is included.

The calculation[5] enabled study of a wider range of parameters (gamma background, counter-cable time constant, and RC-CR filter values) than could be studies experimentally and were extended to include pole-zero networks.[7] The validity of some of the calculations was tested with generators that simulated the gamma noise and the current pulse.

With the noise-to-signal ratio as a criterion, the performance of candidate designs of high sensitivity fission counters were compared to that of the developmental, high temperature unit.[8] The gamma noise spectrum and current pulse amplitude (relative to the high temperature counter) were calculated for various parameters, such as electrode spacing, gas composition, and collection potential. For these calculations, the electrode area of the high sensitivity design was arbitrarily made ten times greater than the high temperature counter to yield a sensitivity of ~10 counts sec^{-1} nv^{-1}. Thus, exposure to the same gamma field would produce a gamma reaction rate which is ten times greater. It also was assumed that the high sensitivity design would be required to operate in a gamma field of 10^5 R/hr, which would be equivalent to 10^6 R/hr for the high temperature

counter, and the gamma noise spectral data obtained from the high temperature counter at 10^6 R/hr were used to predict the spectra for the various candidate high sensitivity designs. After several candidate designs were evaluated, we determined which combination of parameters is important and devised a conceptual design whose performance would almost equal the high temperature fission counter.

2. GAMMA NOISE SPECTRUM MEASUREMENT

The gamma-noise spectrum of a developmental, high-temperature fission counter was obtained by measuring its output voltage with a wide-band, low noise preamplifier and a Rhode and Schwarz selective rf voltmeter at two levels of gamma radiation, 5.8×10^6 and 0.98×10^6 R/hr. The measurement was repeated in the absence of radiation and with no counter voltage to determine the electronic noise (Fig. 1). (These data also included some alpha noise, but because of the enriched ^{235}U used in the counter, the alpha noise did not influence the results of this study.) The sharp decrease at 2.5 MHz in Fig. 1 for both radiation levels was caused by the electronic component of the fission counter current. The ionic component of this current was filtered out by the high-pass RC time constant of the preamplifier used in the measurement.

With the electronic noise subtracted from the gamma noise, there are two additional, less noticeable decreases in the gamma spectrum, one at ~6 and one at >10 MHz. The decrease at 6 MHz was caused by the time constant of the counter capacitance and the impedance of the signal cable. The decrease at >10 MHz was caused by frequency limitations of the high temperature coaxial cable connected to the fission counter.

3. FISSION COUNTER TIME CONSTANT CALCULATION

The time constant is a function of the interelectrode capacitances of the counter and the impedance of the signal cable. For an unguarded counter with only one center electrode, the time constant is the product of the capacitance formed by the electrode and outside shell and of the characteristic impedance of the signal cable.

For guarded counters, such as the developmental, high temperature fission counter, determination of the time constant is more complicated. In the electrical representation of the counter of Fig. 2, the current pulse from the counter is represented by the generator i(t), and the interelectrode capacitance by C_A, C_B, and C_C. Resistor Z_o represents the characteristic impedance of the signal and high voltage cables which are terminated at the preamplifier. The transfer function for the signal-current source to the output at either the high voltage or signal electrode contains a zero and two poles. The zero and one pole occur at extremely high frequencies and do not contribute significantly to the response. The time constant associated with the low frequency pole can be approximated by $2Z_oC_B$, if both C_A and C_C are small relative to C_B. For this developmental counter, the values of C_A, C_B, and C_C are 140, 324, and 3 pF, respectively. With a 50-Ω cable, the time constant of the low frequency pole is 35.9 nsec, giving a breakfrequency of 4.43 MHz.

4. ANALYTICAL PROCEDURES

4.1 RC-CR Filter Optimization

Figure 3 shows the functional models used to optimize the RC-CR filter; Fig. 3a applies to the RC-CR filter alone, and Fig. 3b to the added pole-zero network. In both cases the amplifiers are ideal: they are noiseless, their input impedance is infinite, their output impedance is zero, and their bandwidth is infinite. The inputs for the amplifiers with more

than one input terminal are isolated; the amplifier output is the sum of the input signals. Also, the bandwidth of the preamplifier, which is normally a part of these current-pulse systems, is such that the bandwidth can be neglected without affecting the accuracy of the analysis. This simplifies the expressions for noise and peak voltage.

The analysis is based on a triangular ~~shaped~~ neutron pulse* (Fig. 4), with the power spectral densities of gamma** and electronic noise approximated as $G_\gamma(\omega) = K_\gamma^2/[1 + (\omega/\omega_\gamma)^2]$ and $G_e(\omega) = K_e^2$, where ω_γ represents the breakfrequency (radians/sec) of the gamma noise, and K_γ and K_e are constants relating to the gamma and preamplifier noise, respectively (obtained from Fig. 1).

---

* This pulse shape is based on observations of pulses generated by fission counters with a cylindrical geometry. Such pulses (neglecting bandwidth limitations of the time constant of the signal cable resistance and counter capacitance and the preamplifier) have a fast rise-time to their peak value, followed by a nearly linear decay to zero. The decay time is equal to the electron collection time of the counter, which for ~~this experimental unit~~ the experimental counter is ~50 nsec. The finite rise-time in Fig. 4 was chosen to accommodate the computer solution of the peak voltage expression, and it is small enough to be of no consequence in the subsequent pulse-shaping circuits.

** This approximation would be characteristic of gamma current pulses with an exponential decay time-constant of $1/\omega_\gamma$, or 63.5 nsec. This is an apparent conflict with the assumed triangular ~~shaped~~ neutron current pulse. However, this approximation does yield close agreement to the measured spectrum and justifies its use in this study.

By standard transient analysis techniques, an expression can be determined for the output pulse as a function of the input pulse illustrated in Fig. 4. The time-to-peak value of the output pulse also can be obtained routinely, and its substitution into the expression for the output voltage to determine the peak value yields a complex expression that is most conveniently solved with a computer.

The output contributions of the gamma and preamplifier noise sources can be determined from the transfer functions of the functional models. The equation for the RC-CR filter alone is

$$v_{n\,out}^2 = \frac{T_D}{2}\left[\frac{K_e^2}{T_I\,(T_D + T_I)} + \omega_\gamma^2\, K_1\, K_\gamma^2\right],$$

where $v_{n\,out}^2$ is the mean-square rms output noise; T_D is the differentiating CR time constant; T_I is the integrating RC time constant; K_1 is a factor involving T_D, T_I, T_1, and ω_γ; and T_1 is the fission counter-input cable time constant, $C_D Z_o$. With the pole-zero network, the equation is

$$v_{n\,out}^2 = \frac{T_D}{2}\left[K_2\, K_e^2 + \omega_\gamma^2\, K_3\, K_\gamma^2\right],$$

where K_2 is a factor involving T_D, T_I, T_1, T_2, and T_3; K_3* is a factor involving T_D, T_I, T_1, and T_2; T_2 is the time constant of the zero of the pole-zero network; and T_3 is the time constant of the pole of the pole-zero network.

---

* The time constant T_3 does not appear here, because it was neglected for simplification when the gamma noise contribution was calculated. The assumption was that $T_3 \ll 1/\omega_\gamma$. However, T_3 was retained in the factor K_2 because of the "white" character of the electronic noise spectrum, K_e.

The ratio of the noise and peak voltage expressions, designated N/S, was examined for specific values of the integrating (T_I) and differentiating (T_D) time constants, with a gamma background of 5.8×10^6 R/hr and a counter-cable time constant of 35.9 nsec. These data are plotted in Fig. 5. ~~To show the effect of the counter-cable time constant,~~

To show the effect of the counter-cable time constant on the N/S ratio, a series of data were also calculated for two other arbitrarily selected values of 17.5 and 70.4 nsec. Six values of T_I (5, 15, 25, 35, 55 nsec) were also investigated for each of these two cases, but only the data yielding the best N/S ratios are given here and are shown in Fig 6. For completeness, the best plot of Fig. 5, representing the 35.9 nsec time constant, is repeated in Fig 6.

To determine the effect of gamma background on the filter, N/S ratios were calculated for gamma levels of 0.96×10^6 and 1.0×10^5 R/hr, with a counter-cable impedance time constant of 35.9 nsec. These results are plotted in Fig. 7 along with results from the 5.8×10^6 R/hr case. (Once again, a series of curves for six values of T_I were calculated for each value of gamma background; only the curve showing the best N/S ratio is plotted in Fig. 7.). The values of K_e and K_γ for 0.96×10^6 R/hr were from Fig. 1. The value of K_γ for 10^5 R/hr was computed from the 0.96 R/hr value, with an assumption that the rms gamma background would vary as the 0.5 power of the gamma flux.

Calculations were then made for a pole-zero network added to the RC-CR filter system. Results for a $C_D Z_o$ time constant of 35.9 nsec and a gamma level of 5.8×10^6 R/hr are plotted in Fig. 8 for two values of the zero created by the network; 62.1 and 35.9 nsec. The value of 62.1 nsec was chosen to examine the effect of placing a zero at the break-frequency of the gamma noise of ~2.5 MHz, and 35.9 nsec was chosen to examine the effect of placing a zero at the time constant of the counter and cable impedance. The effect of the pole of the network was also considered. For all preceding calculations, the value of the pole was arbitrarily selected as 0.1 the value of the zero. The effect of doubling the value of the pole is shown also in Fig. 8. (These curves, again in each

case, represent the best of six values of the time constant, T_I)[8]

4.2 HIGH SENSITIVITY FISSION COUNTER

The N/S ratios of the candidate high sensitivity fission counters designs were computed from the same expressions for noise (RC-CR filter only) and the pulse amplitude derived {as explained} in Section 4.1. However, the shapes of the gamma noise spectrum and the current pulse changed as the design deviated from that of the developmental, high temperature counter.

4.2.1 Influence on the Gamma Noise Spectrum

The breakfrequency ω_γ is assumed to vary inversely as the electron collection time, T_c, and it can be determined for high sensitivity counter designs by comparing it with the breakfrequency of the high temperature counter at 2.5 MHz. For example, if the collection time of the high sensitivity counter is made twice as long as that of the high temperature counter, the breakfrequency of the high sensitivity counter is $0.5\,(2\pi)\,(2.5 \times 10^6)$.

The low frequency value of the power spectral density, K_γ^2, can be derived for the high sensitivity counter designs by applying the following expressions,*

$$K_\gamma = \sigma_\gamma / (\Xi W_\gamma)^{1/2} \quad ,$$

$$\sigma_\gamma = K_1 \bar{Q}_\gamma (R_\gamma / T_c)^{1/2} \quad ,$$

$$\Xi W_\gamma = \tfrac{1}{2} (1/T_c) \quad ,$$

*The expression for σ_γ was obtained by applying Campbell's theorem to the triangular pulse of Fig. 4 for a peak amplitude of $Q_\gamma Z_o / T_c$ and a mean reaction rate R_γ.

where σ_γ is the rms gamma noise [redacted]; BW_γ, the bandwidth of gamma noise in radians/sec; R_γ, the gamma reaction rate; $\bar{Q}_\gamma$ the average charge per gamma event; and K_1 and K_2 are constants of proportionality. Then, if one assumes the same gamma reaction rate for the high temperature and high sensitivity counters, the following expression is derived:

$$K_{\gamma(HS)} = \left\{ \sigma_{\gamma(HT)} / \left[BW_{\gamma(HT)} \right]^{\frac{1}{2}} \right\} \left[\bar{Q}_{\gamma(HS)} / \bar{Q}_{\gamma(HT)} \right]$$

where HS and HT refer to high sensitivity and high temperature.

The ratio $\sigma_{\gamma(HT)} / \left[BW_{\gamma(HT)} \right]^{\frac{1}{2}}$, which is $K_{\gamma(HT)}$, is obtained from the measured data in Fig. 1. Constants K_1 and K_2 do not appear in the expression for $K_{\gamma(HS)}$ because, in its development, these constants are cancelled in the ratio of $K_{\gamma(HS)}$ to $K_{\gamma(HT)}$.

4.2.2 Normalization of the Magnitude of the Current Pulse

As the collection time or electrode spacing, or both, was varied in the various candidate designs, the pressure of the gas-filling in the counter was adjusted to control the charge generation so that the amplitude of the current pulse would be constant. This procedure normalized the amplitude of the current pulse and required control of $\bar{Q}_\gamma$ so that the adjusted gas pressure appropriately would affect the value of K_γ for the gamma noise spectrum. For example, to design a high sensitivity counter with an electrode spacing four times and a collection time twice the values of the high temperature counter (as in HS-5), the gas pressure was decreased to 0.5 that of the high temperature counter. This doubled the

charge generation* and kept the magnitude of the current pulse constant. This required a doubling of the value of $\bar{Q}_{\gamma\,(HS)}$ and, hence, $K_{\gamma\,(HS)}$.

---

* The following simple relationships were used: $v_d = K_3\, E/P = K_3\, V/SP$; $V = S^2\, P/T_c$; $T_c = S/v_d = 1/K_3\,(S^2\, P/V)$; and $\bar{Q} = K_4\, PS$

In these equations, T_c is the electron collection time; v_d, drift velocity; V, bias voltage; E, electric field; $\bar{Q}$, charge per ionizing event; S, electrode spacing; P, pressure; and K_3 and K_4, constants. Since we were comparing counters which were assumed to follow these same relationships; K_3 and K_4 were made equal to unity, and they do not appear elsewhere in this study.

5. EXPERIMENTAL PROCEDURES

5.1 Integral Bias Measurements with the Developmental Fission Counter

Integral bias measurements were made with the developmental, high-temperature fission counter exposed to two levels of gamma background, 5.8×10^6 and 0.98×10^6 R/hr. Each measurement was repeated with four values of RC-CR filters in the main amplifier. In each case, the integrating and differentiating time constants had equal values of 15, 20, 17 and 36 nsec.

Integral bias measurements with each filter were then made with the counter exposed to a neutron source. The procedure was duplicated with all nuclear radiation sources removed to determine the electronic noise background.

With the data from these measurements, the curves in Fig. 4 were obtained with a single curve representing the neutron integral bias measurement for all filters, ~~neutron integral bias curve represents the data obtained with the four filters.~~ To create Fig. 9, each set of data (electronic noise, electronic plus gamma noise, and neutron integral bias) associated with a particular filter was first plotted on one set of coordinates, using log scales for both the count-rate and discriminator coordinates. All plots were then superimposed and adjusted horizontally (along the discriminator coordinates) so that the neutron integral bias curves coincided precisely. As a result, the relationship of all curves in Fig. 9 was established correctly.

5.2 Measurements with Simulated Neutron Pulses and Gamma Noise

To verify the analytical optimization of the RC-CR filter and the effect of a pole-zero network on the performance of current-pulse counting systems, measurements were made with simulated neutron pulses and gamma noise. To reduce the complexity of the experimental setup, both signals were simulations of those that would normally appear at the output of the fission counter-cable time constant $C_D Z_o$, as shown in Fig. 3.

The neutron pulse was simulated by a Berkeley BH-1 pulse generator, with rise and fall time settings of 50 nsec. The shape of this pulse was similar to pulses obtained from the developmental fission counter and cable assembly.

The gamma signal was simulated by a CODI diode (CODI Semiconductor Division of Computer Diode Corp.) as a noise source. By adjustment of the diode current and breakfrequency, a close approximation to the power spectral-density function of the gamma noise was generated. (For further simplification, only the break at 2.5 MHz was reproduced.) The simulated gamma signal output from the generator appeared as a current source and was applied along with the simulated neutron pulse into the 50-Ω input of a wide-band preamplifier that preceded the main amplifier system and filter network.

During a measurement, the gain of the main amplifier was adjusted until the peak output signal was the same for each filter time-constant under test; then a simulated neutron pulse with the same amplitude was fed to the input of the preamplifier. The discriminator threshold required to yield a 2500 count/sec background was recorded (Table 1). This technique of measuring a single point instead of several points on the noise curve to determine the entire noise curve was chosen for convenience.

6. RESULTS AND DISCUSSION

6.1 RC-CR Optimization

6.1.1 Effect of Fission Counter-Cable Time Constant ($C_D Z_o$) on Filter Design

Figure 5, with 5.8×10^6 R/hr and 35.9 nsec for the gamma background and counter-cable time constant, respectively, shows minimum values of N/S ratios*

---

* The N/S units are arbitrary, and only relative significance should be attached to them in all figures where they are shown.

that are nearly equal over a wide range of time constants. The minimum ratios for T_I equal to 15 and 25 nsec are slightly less than the others and are very close to the N/S ratios obtained when T_I equals T_D ($T_D/T_I = 1$).

For a $C_D Z_o$ time constant of 17.5 nsec, Fig. 6 shows a significant improvement of the N/S ratios over those obtained with a time constant of 35.9 nsec. Examination of the specific noise and signal amplitude data (not given here) shows that, although the noise is greater for the 17.5 nsec value, it is offset by an increase in the signal amplitude, yielding an improved N/S ratio.

As the $C_D Z_o$ time constant is increased to 70.4 nsec, Fig. 6 shows a significant increase of the N/S ratio. Examination of the specific data of noise and signal (not given here) yields information not apparent in the N/S ratio; i.e., with the longer time constant of 70.4 nsec the noise voltage is less than with a time constant of 35.9 nsec. The higher N/S ratio is a result of a greater reduction in the signal amplitude.

6.1.1 Effect of Gamma Background on Filter Design

Figure 7 shows the effect of the gamma background on the N/S ratio and a trend to higher values of T_I for the best ratio is apparent as the gamma background is reduced. This result is as expected since the low-frequency content of the noise spectrum is less with a reduction of the gamma background. Larger values of T_I create poorer N/S ratios because of a loss of signal amplitude. The shift of the curves to smaller values of N/S as the gamma level is lowered also is as expected because of the reduction of input noise.

This calculated data of Fig. 7 compare favorably with the experimental data shown in Fig. 9. The experimental data indicate that best RC-CR time constant (with $T_I = T_D$) is either 15 or 20 nsec for a 5.8×10^6 R/hr gamma background and either 27 or 36 nsec for a 0.96×10^6 R/hr gamma background. The data of Fig. 7 show values of T_I of 15 and 25 nsec respectively for these two gamma backgrounds.

6.1.3
6.3 Effect of the Pole-Zero Network

Figure 8 summarizes analytical data that show the effect of the pole-zero network on the N/S ratio. As in Sect. 6.2, the counter-cable time constant was 35.9 nsec, and only the 5.8×10^6 R/hr gamma background was considered. Each curve in Fig. 8 represents the best of six values of T_I (5, 15, 25, 35, 45 and 55 nsec).

Two positions of the zero were considered: one at the breakpoint of the gamma noise spectrum (62.1 nsec), and the other at the counter-cable time constant (35.9 nsec). In each case, the associated pole was arbitrarily placed at 0.1 the value of its zero. The minimum N/S ratios for both cases, 4.5 units, respectively, are both significantly higher (poorer) than the 4.1 units for the RC-CR filter alone, as shown in Fig. 5. Some insight into the performance of the pole-zero network also can be obtained by examination of specific signal and noise data. Compared to data for the RC-CR filter acting alone, there is nearly a factor of 2 enhancement of the signal; however, this is more than offset by an enhancement of noise.

The position of the pole of the network does significantly affect the N/S ratio, as seen in Fig. 8 where the value of the pole is increased to 12.4 nsec. Even though there is some improvement of the N/S ratio, it is still less than with the RC-CR filter alone. Values for this pole greater than 12.4 nsec did not yield any additional improvement.

Table 1 shows that a pole-zero network with a 50-nsec, RC-CR filter has a 2500-count/sec noise threshold of 344 discriminator divisions; an RC-CR filter alone with a 27-nsec time constant has a 2500-count/sec threshold of 355. This apparent improved performance by the pole-zero network contradicts the analytical data described previously. The difference possibly can be explained as follows: a 2-nsec RC time constant was omitted in the noise expression to simplify the calculations, but was retained in the main amplifier to obtain the data of Table 1. (This RC time constant is used to suppress the effects of

high-frequency resonances that occur in the RC-CR filter.) Also, inaccuracies in the shape of the spectrum of the gamma noise generator could have caused some of the observed error.

The result of the analysis of the time constant involving the interelectrode capacitances of the counter and the impedance of the signal cable is very significant. It shows how either guarded or differential operation of a two-electrode fission counter effectively increases the contribution of the capacitance existing between the electrodes to this time constant. The mechanism involved is similar to that of the Miller effect.

5.2 High Sensity Fission Counter Design

The ratios of noise-to-peak voltage (N/S) were determined for 13 designs of the high sensitivity fission counter, and these ratios were compared with that of the high temperature counter design to establish a level of performance. As an example, the first design, HS-1, was identical to the high temperature counter except that the HS-1 electrode area was ten times greater. (This tenfold increase in area was retained in all HS designs to yield the additional sensitivity.) The N/S ratio of the HS-1 design was 3.08 times higher (poorer) than the high temperature counter.

Table 2 is a tabulation of the various designs. All parameters in this table were normalized to the high temperature counter (HT-1 in Table 2) for comparison and evaluation. The table also lists the optimum time constant for an RC-CR filter ($T_I = T_D$) in each case. In agreement with the work with RC-CR filters, the best N/S ratio was obtained when the RC-CR filter time constants were equal, or very nearly so.

The first three counters were designed to learn how counter capacitance alone would influence the N/S ratio. This capacitance was controlled by the adjustment of the electrode spacing, and the collection time and the charge were held at the same value as the high temperature design by adjusting the filling-gas pressure. As expected, the N/S ratios for

HS-1, HS-2, and HS-3 improved as the capacitance was made smaller; however, at best, the ratio was still a factor of 1.52 poorer than the high temperature counter, with four times more bias voltage required.

Next, we wished to determine whether a faster counter would yield a better N/S ratio. The HS-4 counter was designed with one-half the collection time of the high temperature counter. The results show that the N/S ratio was more than a factor of 3 poorer than the HT-1 counters and was also poorer than the HS 2 design which was identical to the HS-4 counter except for a longer collection time. We concluded that the integrating effect of the counter capacitance-cable impedance time constant is so severe on a fast pulse that no advantage is derived from the larger values of the current pulse so obtained. The difference in the noise signals for the HT-1 and the HS-4 counters (data not given here) is insufficient to explain this change in the N/S ratio.

Since it appeared that the peak voltage signal had a dominant influence on the ratio, we decided that longer collection times (with the charge per ionizing event increased proportionately for normalization) and less electrode capacitance might yield a better ratio. Thus, the HS-5 counter was designed to test this assumption, and its N/S ratio was only 21% poorer than for the HT-1. However, the drift velocity for the HS-5 design (and also of HS-2, -3, and -4) is physically unrealizable.

Designs HS-6 through HS-12 were attempts to achieve a performance equal to or superior of that of the HS-5 counter, but with a realizable drift velocity. The electrode spacings in HS-6, -7, and -8 were twice as wide as in the reference counter HT-1, and the collection times were made progressively longer from HS-6 to HS-8. The spacing for HS-9, -10, -11, and -12 was increased to four times that of HT-1, and the collection time for these units was progressively increased as well.

An interesting change in the N/S ratios of HS-6 to -12 was observed as the collection time was increased and with the charge per pulse correspondingly increased to normalize the current-pulse amplitude. The N/S ratios improved, and both the ratio and the value of the optimum RC-CR time constant approached limiting values.

We believe that an explanation of this effect lies in the noise spectrum created by the analytical procedure and the amplitude of the output pulse of the filter as related to the linear decay of the input pulse. The triangular input pulse becomes almost a step function as its linear decay time is lengthened by making the collection time longer. If the counter-cable time constant is neglected (which is reasonable, particularly for the HS-9, -10, -11, and -12 counters), the peak amplitude of the output pulse from the filter (for equal RC-CR time constants) will be nearly constant for all values of this filter time constant. The noise spectrum created by the procedure which shifts ω_γ as a linear function of $1/T_c$ (and with K_γ adjusted to normalize $\bar{Q}_\gamma$) will always retain the same "noise corner" (i.e., the intersection of the gamma and electronic noise spectra), once again neglecting any effect of the counter-cable time constant.

For this characterization of noise and signal, the optimization problem approaches the classic one which has been treated previously.[3-5] The time constant of the optimum RC-CR filter will be consistent with corner frequency, and the N/S ratio will reach some limiting value.

As a consequence, in the application of the high sensitivity counter for liquid-metal fast breeder reactors, some trade-off of the N/S ratio may be required for counting resolution. Thus, HS-10, with a collection time four times that of the HT-1 (giving a value of ~200 nsec) would appear to be a reasonable compromise except for one limitation: this counter would require an operating voltage four times that of HT-1 or ~1600V. Even split, high voltage operation of the counter (assuming a guarded structure) would require an undesirably high voltage.

We considered filling the counter with a faster gas mixture to achieve a lower operating voltage. The high temperature counter (HT-1) was designed with an argon-nitrogen mixture to obtain good long-term stability at high temperatures. The high sensitivity counter, not required to operate at these high temperatures, could advantageously use a faster mixture, such as Ar-5% CO_2. The HS-13 counter is the same as the HS-10 counter except that its gas is Ar-5% CO_2. The voltage of 1.2 kV for HS-13 (vs 4 for HS-10, Table 2) implies an operating voltage of 1.2 x 400, or 480V, a reduction by a factor of 3.3 from the operating voltage of the design with an argon-nitrogen gas.

~~times less with the faster Ar-5% CO_2 gas. (This result is also observed for the HT-2 counter, which is identical to the reference counter HT-1 except that the gas filling is Ar-CO_2 in the HT-2 counter.)~~

7. CONCLUSIONS

The analytical study of RC-CR filters shows that when the fission counter-cable time constant is increased, with other parameters unchanged, the gamma rejection capability of the counter is reduced. The cause appears to be a loss of amplitude of the neutron pulse which more than offsets a corresponding reduction of gamma noise. The analysis is proved valid by the good correlation of results from measurements obtained with a fission counter operating in a gamma background.

The optimum value of RC-CR filter time constant changes with the gamma background; its value increases as the gamma background is reduced.

A pole-zero network added to the amplifier of a current-pulse system, with its zero positioned near the counter-cable time constant, requires optimization of both its associated pole and an RC-CR filter to obtain the most favorable rejection of gamma noise. At best, however, it does not exceed the performance of an RC-CR filter alone.

The guarded or differential operation of a two-electrode fission counter increases the effective value of the capacitance existing between the electrodes.

Design of a fission counter with a sensitivity of 10 counts sec^{-1} nv^{-1} is feasible. Its performance in a gamma background of 10^5 R/hr would be almost as good as that of a high temperature counter[1] at 10^6 R/hr. Its construction would be similar to that of the high temperature counter. Its electrode area would be 10^4 cm^2 and its electrode spacing 6.08 mm (0.24 in.) The gas mixture would be Ar-5% CO_2 at a total pressure of ~760 torr. The operating voltage would be 480 V. For a current-pulse mode of operation, an RC-CR filter with a 40 nsec time constant would yield the best performance at 10^5 R/hr gamma background.

8. ACKNOWLEDGMENTS

I wish to express my appreciation to C. H. Nowlin for his advice and encouragement to explore the possibilities of pole-zero cancellation in this study and to V. K. Paré and H. N. Wilson (all of ORNL) for their painstaking review of this paper. Particular thanks are also due to Dr. T. V. Blalock of the Electrical Engineering Department of the University of Tennessee for his help in the analytical phase of the study. Much appreciation is also expressed to R. L. Simpson and J. M. Jansen (ORNL) for their assistance in writing the programs for the computer computations of the noise-to-signal ratios.

9. REFERENCES

1. D. P. Roux et al., "A Neutron Detection System for Operation in Very High Gamma Fields," *Nucl. Appl. Technol.* 9(5), 736 (1970).

2. V. K. Paré, W. T. Clay, J. T. De Lorenzo, and G. C. Guerrant, "Design Parameters and Test Results for a Fission Counter Intended for Operation up to 750°F at High Gamma Dose Rates;" presented at 1974 Nucl. Sci. Symp., Washington, D.C., Dec. 11–13, 1974. (To be published in *IEEE Trans. Nucl. Sci.*, 1975.)

3. M. Tsukuda, "Pulse Analyzing System for a Gridded Ionization Chamber," *Nucl. Instrum. Methods* 14(3), 241 (1962).

4. T. V. Blalock, *Optimization of Semiconductor Preamplifiers for Use with Semiconductor Detectors*, ORNL-TM-1055 (Feb. 1965).

5. A. B. Gillespie, *Signal, Noise and Resolution in Nuclear Counter Amplifiers*, Pergamon Press, London, 1953.

6. J. T. De Lorenzo, "Optimization of RC-CR Filters for Processing Current Pulses from a Fission Counter Operating in a High Gamma Background," ORNL-TM-4932 (Aug. 1975)

7. C. H. Nowlin and J. L. Blankenship, "Elimination of Undesirable Undershoot in the Operation and Testing of Nuclear Pulse Amplifiers," *Rev. Sci. Instrum.* 36(12), 1830 (1965).

8. J. T. De Lorenzo, "Feasibility Studies for a High Sensitivity Neutron Counter," ORNL-TM-5123 (to be published).

10. APPENDIX

10.1 The Transfer Function of a Guarded Fission Counter

From Fig. 2 it can be shown that the transformed expression for the voltage appearing at the signal electrode is

$$V_{sig}(s) = I(s)\, K \frac{(s + a)}{(s + b)\,(s + c)} ,$$

where

$$K = \frac{Z_o \tau_3}{\tau_1\tau_3 + \tau_1\tau_2 + \tau_2 + \tau_3} ,$$

$$\tau_1 = Z_o C_1 ,$$

$$\tau_2 = Z_o C_2 ,$$

$$\tau_3 = Z_o C_3 ,$$

$$a = 1/\tau_3 ,$$

$$b = \frac{(\tau_1 + 2\tau_2 + \tau_3) - (\tau_1^2 + 4\tau_2^2 + \tau_3^2 - 2\tau_1\tau_3)^{1/2}}{2\tau_1\tau_3 + 2\tau_1\tau_2 + 2\tau_2\tau_3} ,$$

$$c = \frac{(\tau_1 + 2\tau_2 + \tau_3) + (\tau_1^2 + 4\tau_2^2 + \tau_3^2 - 2\tau_1\tau_3)^{1/2}}{2\tau_1\tau_3 + 2\tau_1\tau_2 + 2\tau_2\tau_3} .$$

~~By examination of~~ From the expressions for b and c, it ~~can be seen~~ follows that if $\tau_1 << \tau_2 >> \tau_3$, then $b \approx 1/2\tau_2$ and $c \approx 2/(\tau_1 + \tau_3)$ and the transient response will be dominated by the low frequency pole, $1/2\tau_2$.

The transformed expression for the voltage appearing at the high voltage electrode is ~~given as~~ $V_{HV}(s) = I(s)\, K_o\{(s + d)/[(s + b)\,(s + c)]\}$. With the exception of polarity, the expression is identical to that for the signal electrode. K_o and d have the same form as K and a, with τ_1 and τ_3 interchanged.

10.2 The Peak Voltage Expression for the N/S Ratio

10.2.1 RC-CR Filter

The solution for the peak voltage transmitted by the model of Fig. 3a for a triangular input pulse (Fig. 4) can be simplified by analyzing the first differential of the input pulse as shown in Fig. 10.

The first differential can be represented by three steps: $(1/t_1)\ U(t)$, $-[t_2/t_1\ (t_2 - t_1)]\ U(t - t_1)$, and $[1/(t_2 - t_1)]\ U(t - t_2)$. The transient response of the model is obtained for this first differential, and the result is integrated to derive the desired response for the triangular pulse. The transient response for the first differential, when equated to zero, can be solved to determine the time to the peak of the output pulse. This value of time, when substituted into the transient response for the triangular pulse, will yield the peak voltage for a particular set of parameters in the model.

10.2.2 RC-CR Filter with Pole-Zero Network

The procedure is identical to that previously described, with the addition of the pole-zero network response to the overall transfer function. The gain G of the amplifier following the network is made equal to τ_2/τ_3 to normalize the gain of this model for those two parameters of the pole-zero network.

10.3 The Noise Expression for the N/S Ratio

The mean-square noise voltage at the output of the models of Fig. 3 is

$$V^2_{n\ out} = \frac{1}{2\pi} \int_0^\infty G_e f^2_e(\omega)\ d\omega + \frac{1}{2\pi} \int_0^\infty G_\gamma f^2_\gamma(\omega)\ d\omega\ ,$$

where $f_e(\omega)$ and $f_\gamma(\omega)$ are the sine-wave frequency responses of the model for the electronic noise and gamma noise, respectively.

For the RC-CR filter model,

$$f_e^2(\omega) = \frac{\omega^2\tau_D^2}{(1 + \omega^2\tau_D^2)(1 + \omega^2\tau_I^2)}$$

and

$$f_\gamma^2(\omega) = \frac{\omega^2\tau_D^2}{(1 + \omega^2\tau_1^2)(1 + \omega^2\tau_D^2)(1 + \omega^2\tau_I^2)} .$$

For the model with the pole-zero network added,

$$f_e^2(\omega) = \frac{\omega^2\tau_D^2(1 + \omega_2^2)}{(1 + \omega^2\tau_3^2)(1 + \omega^2\tau_D^2)(1 + \omega^2\tau_I^2)}$$

and

$$f_\gamma^2(\omega) = \frac{\omega^2\tau_D^2(1 + \omega^2\tau_2^2)}{(1 + \omega^2\tau_1^2)(1 + \omega^2\tau_3^2)(1 + \omega^2\tau_D^2)(1 + \omega^2\tau_I^2)} .$$

To simplify the analysis involving $f_\gamma^2(\omega)$, the factor $(1 + \omega^2\tau_3^2)$ was omitted. This was justified on the basis that τ_3, which is the time constant of the pole of the pole-zero network, is $\ll 1/\omega_\gamma$.

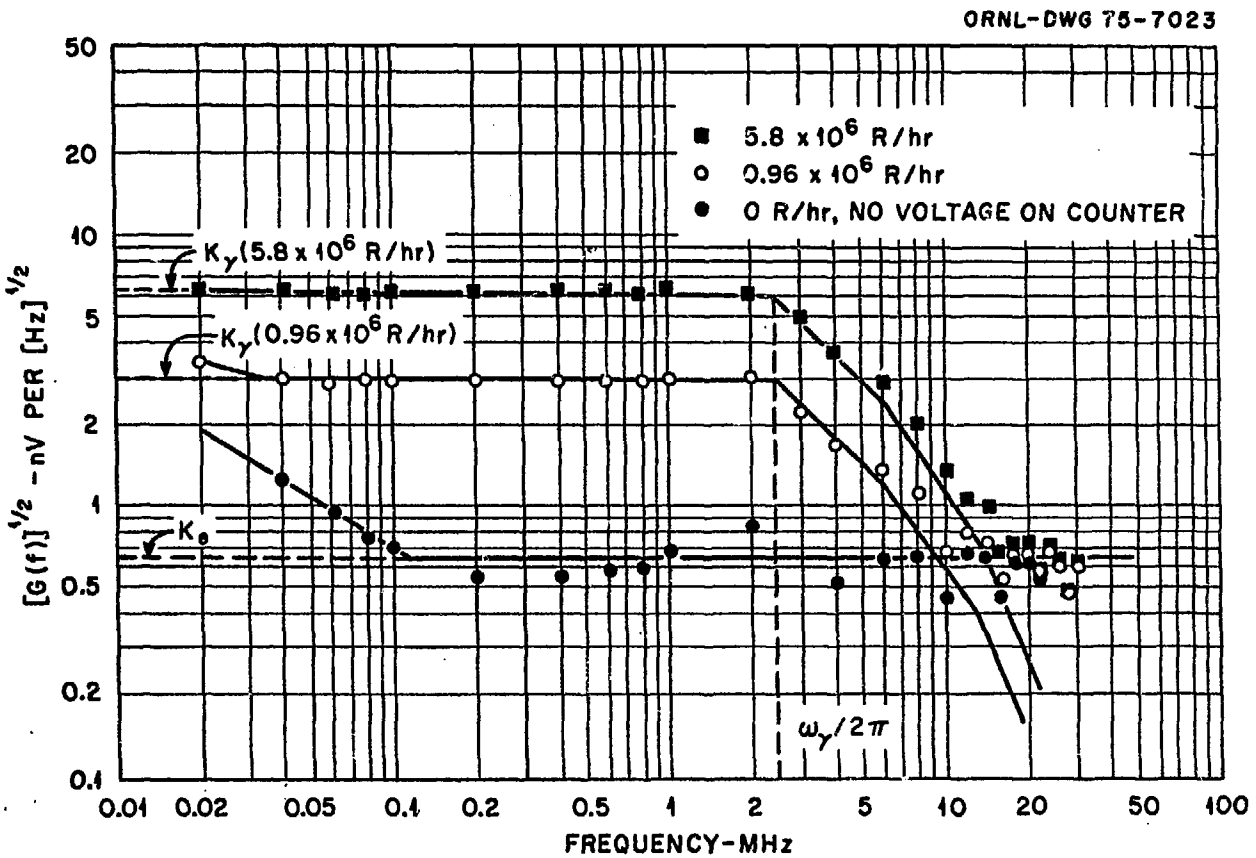

Fig. 1. Gamma pile-up spectral noise density for high temperature fission counter.

ORNL-DWG 75-7024

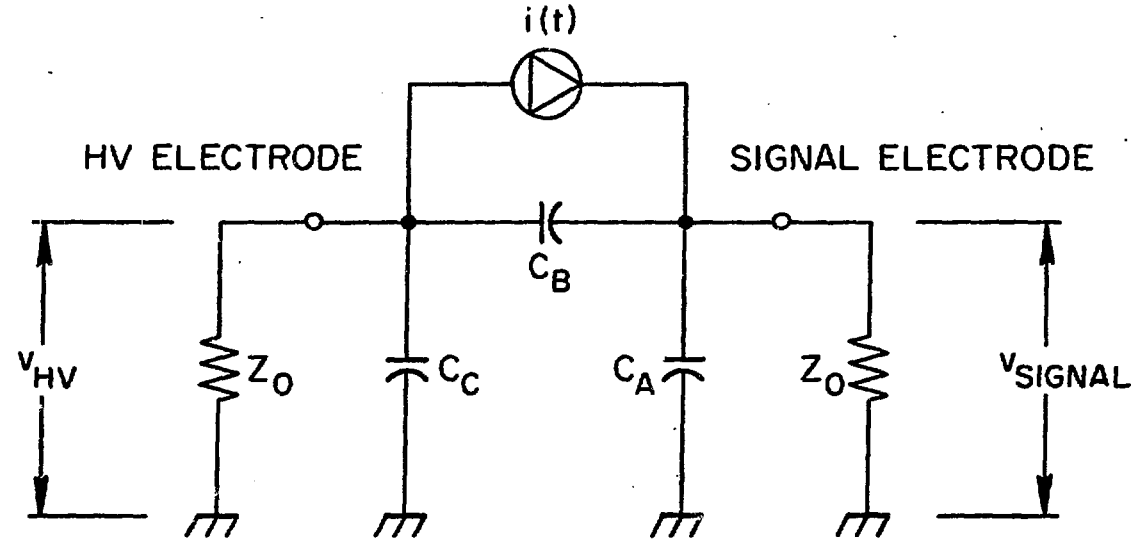

REPRESENTS THE OUTSIDE SHELL OF THE COUNTER

$$\frac{V_{SIG}(s)}{I(s)} = K\frac{(s+a)}{(s+b)(s+c)}$$

$$\frac{V_{HV}(s)}{I(s)} = K_O\frac{(s+d)}{(s+b)(s+c)}$$

Fig. 2. Electrical equivalent of fission counter.

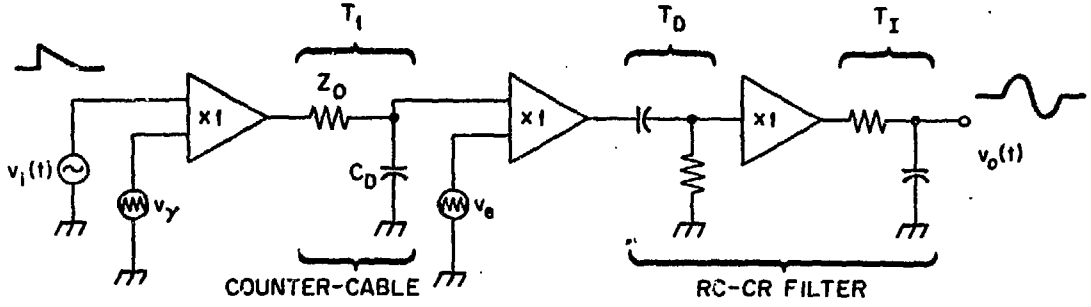

(a) RC-CR FILTER

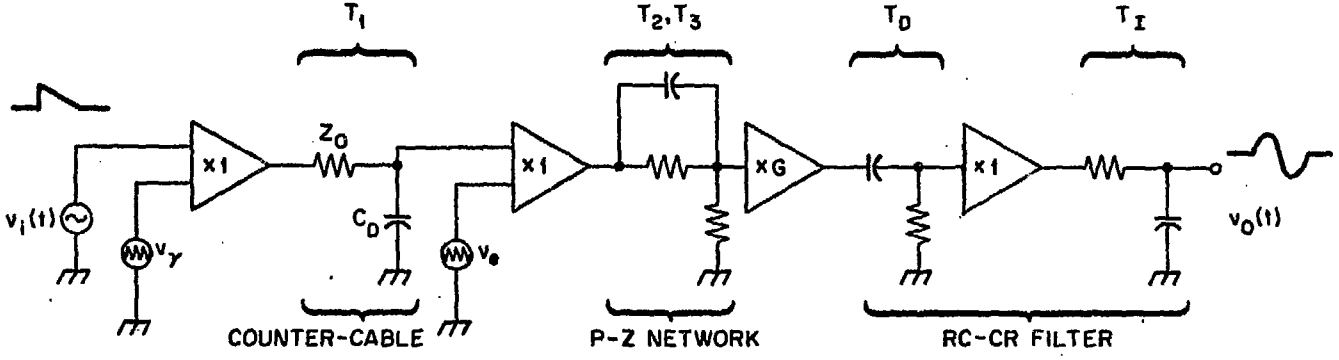

(b) RC-CR FILTER WITH POLE-ZERO NETWORK

Fig. 3. Models used in analysis.
a. RC-CR filter
b. RC-CR filter with pole-zero network

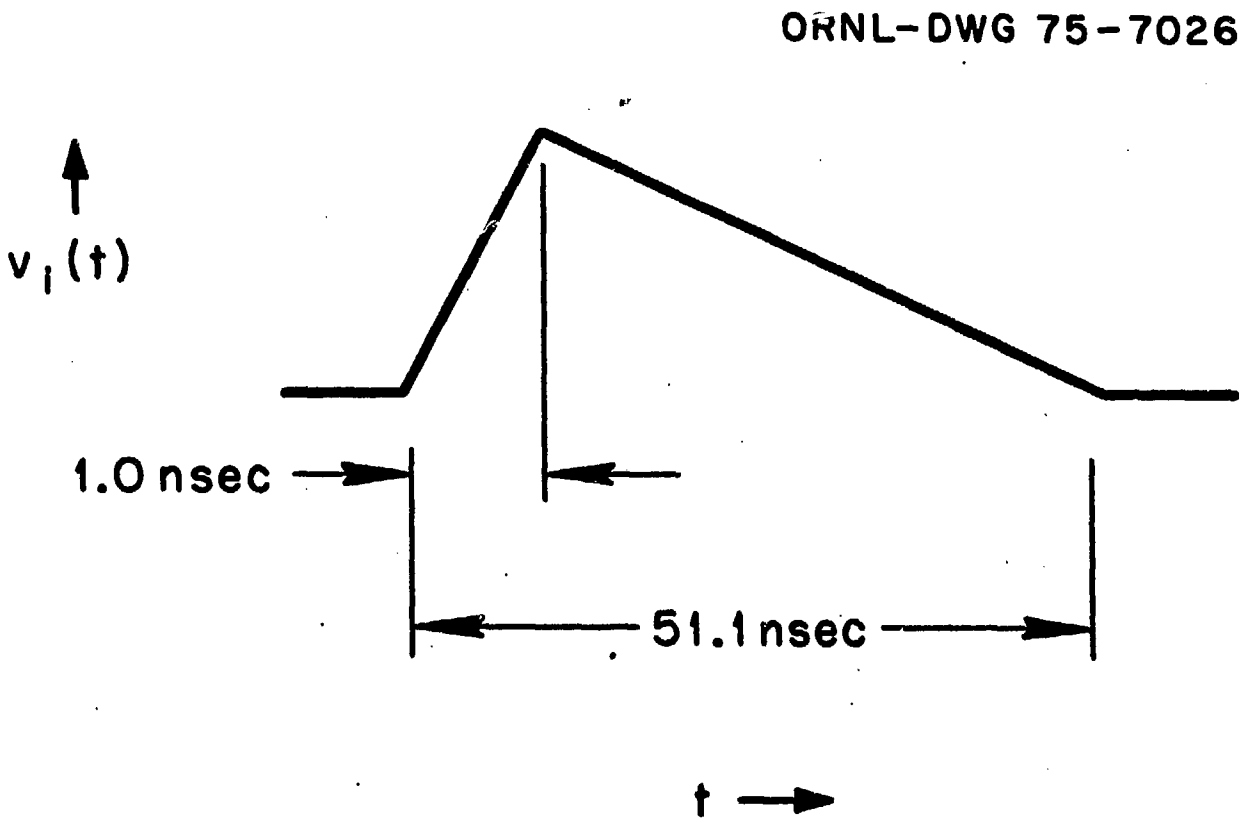

Fig. 4. Input pulse shape used in analysis.

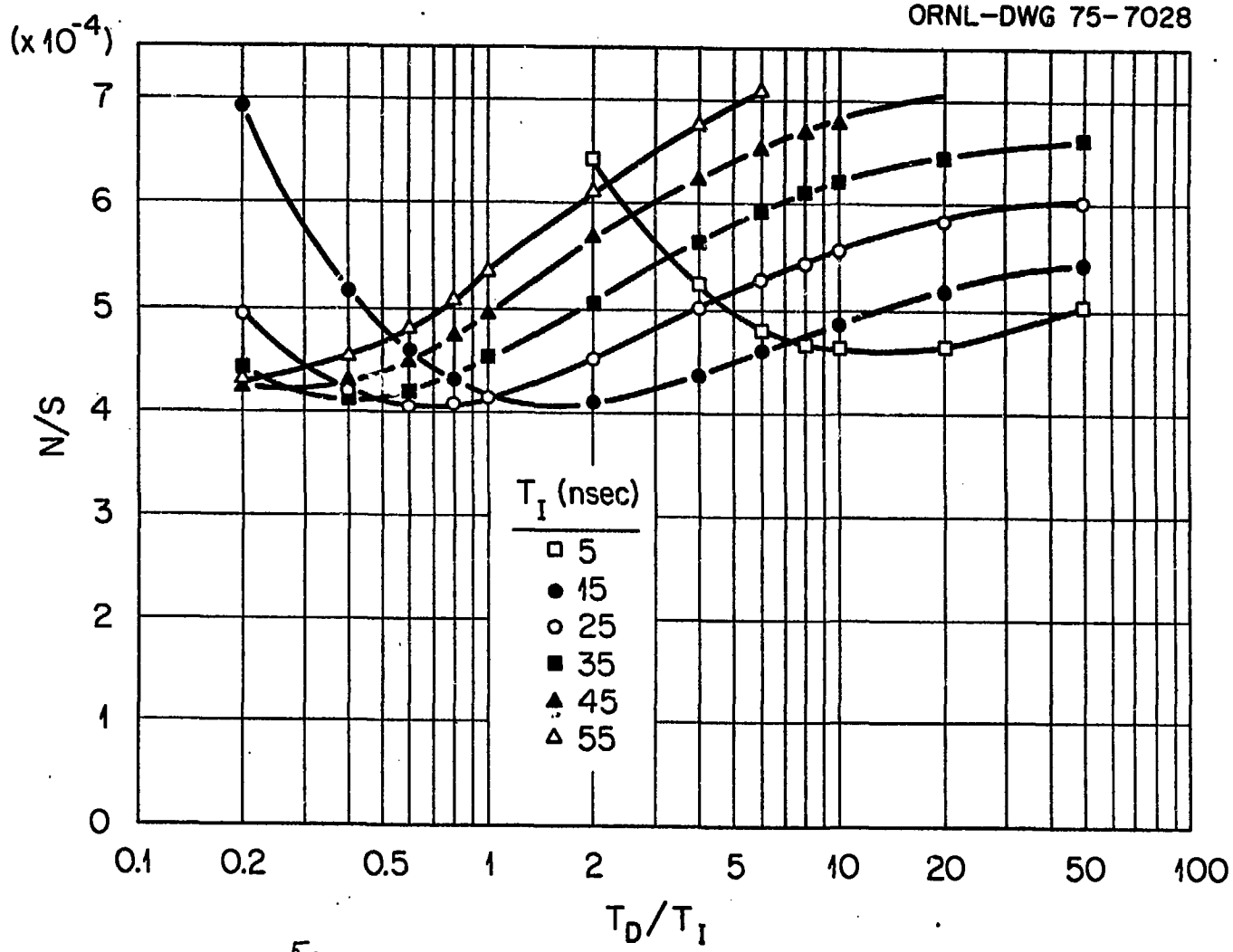

Fig. 5. N/S with RC-CR filter, $C_D Z_o$ = 35,9 nsec, and gamma background=5.8 × 10^6 R/hr.

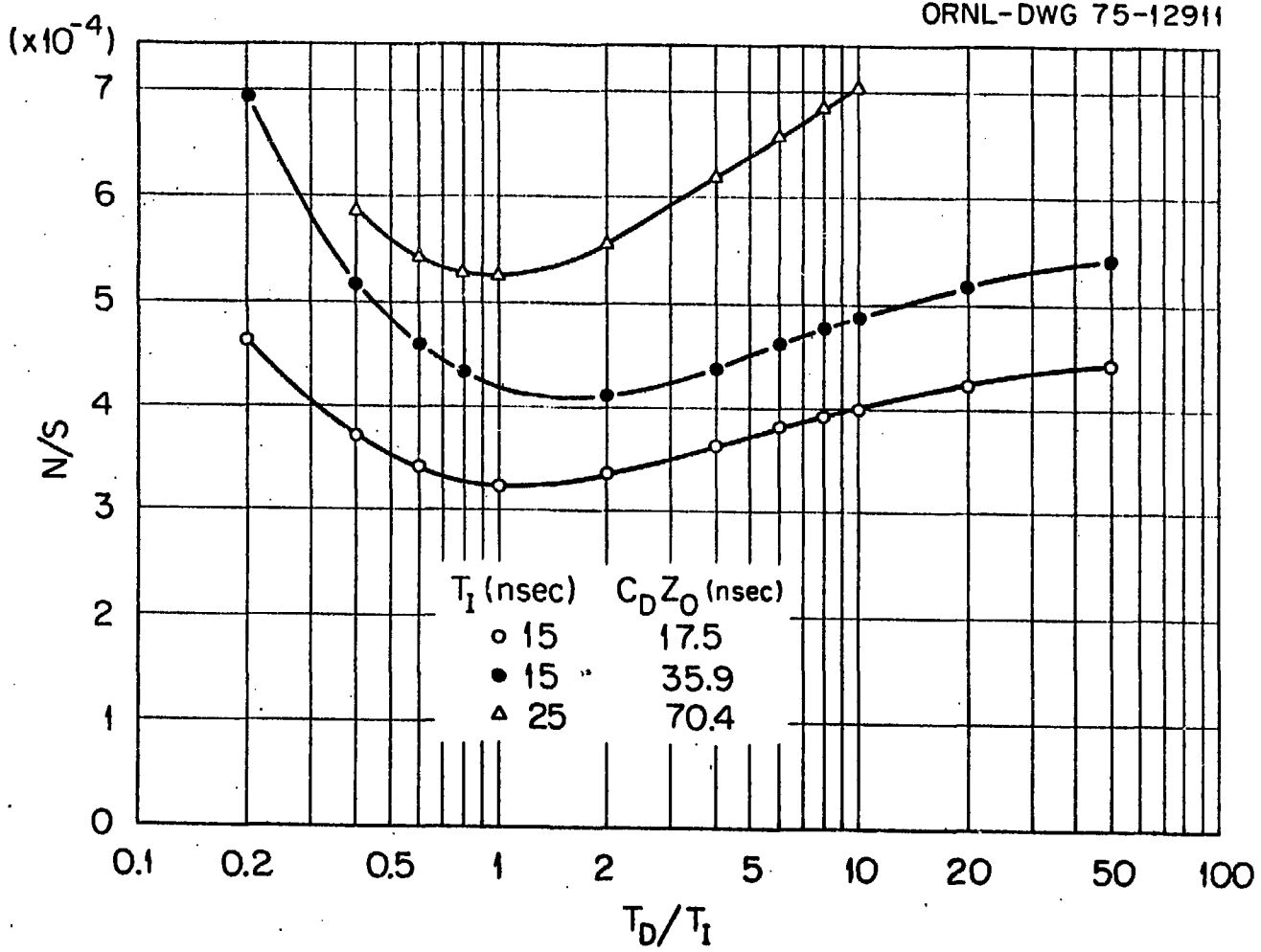

Fig. 6. Effect of counter-cable time constant ($C_D Z_o$) on RC-CR filter with gamma background = 5.8×10^6 R/hr.

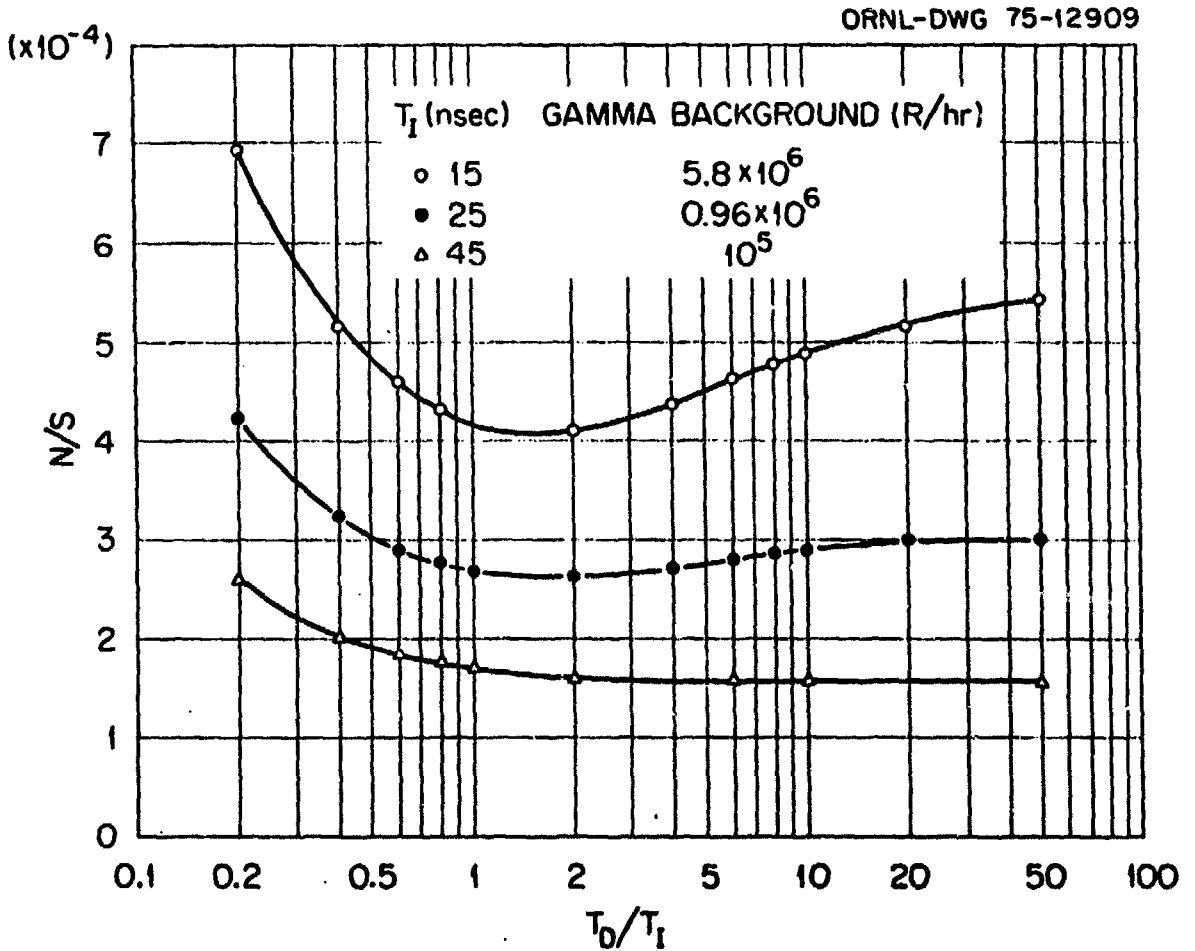

Fig. 7. Effect of gamma background on RC-CR filter with $C_D Z_o = 35.9$ nsec.

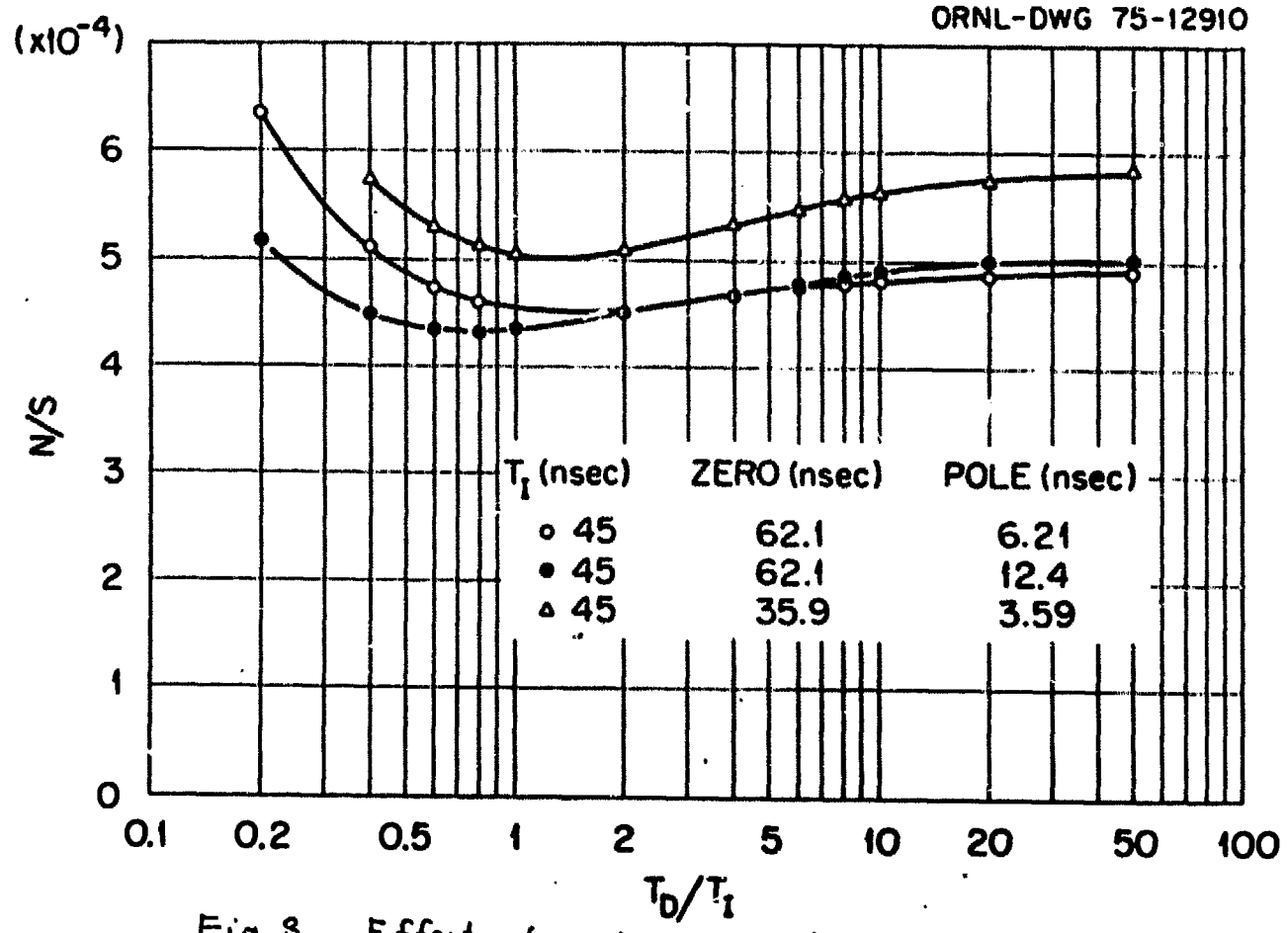

Fig. 8. Effect of pole-zero network with C_{D2} = 35.9 nsec and gamma background = 5.8 x 10^4 R/hr.

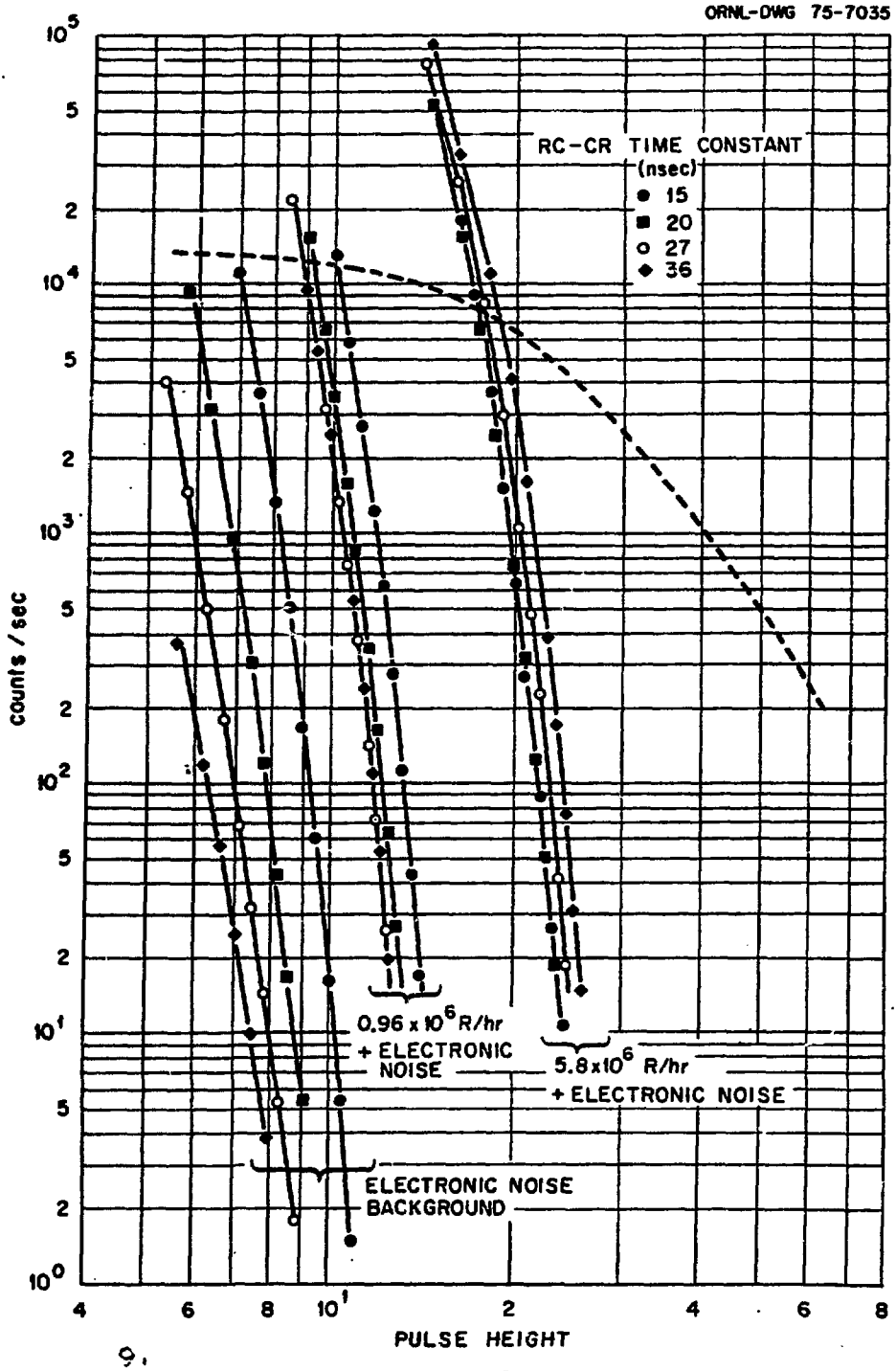

Fig. 9. Integral bias response for a high temperature fission counter.

ORNL-DWG 75-9857

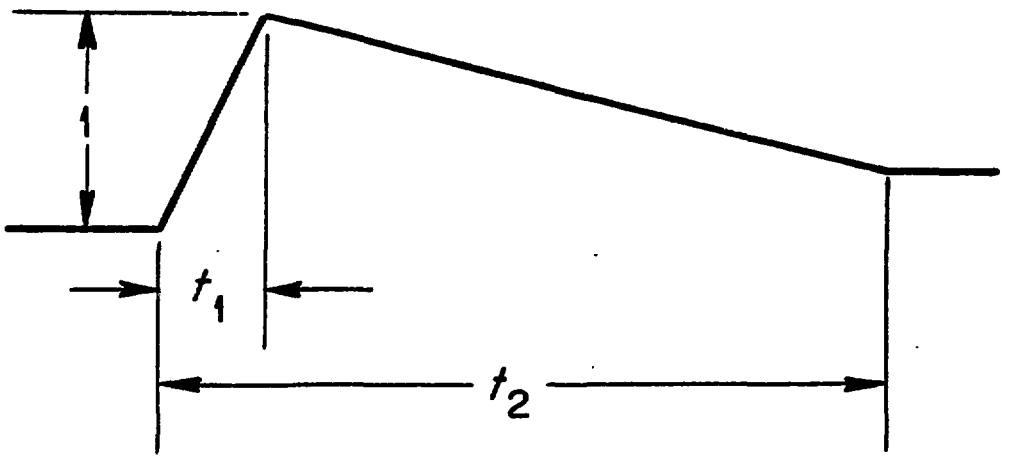

(a) INPUT PULSE

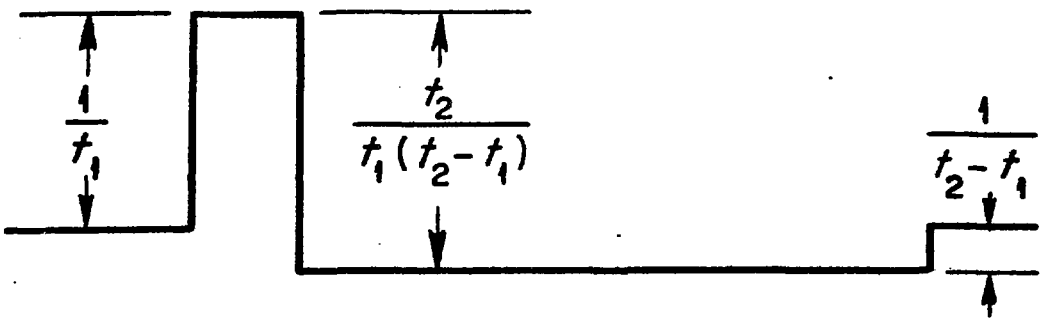

(b) FIRST DERIVATIVE OF INPUT PULSE

Fig. 10. General input pulse shapes used to obtain the peak voltage expression.

Table 1. Summary of measurements with simulated gamma noise

RC-CR Filter Time Constant (nsec)	P-Z Network[a]	High Frequency RC Filter Time Constant (nsec)	Discriminator Threshold for 2500 counts/sec (divisions)
20	None	2	360
20	None	13	350
20	None	27	354
27	None	2	355
27	None	20	358
27	None	36	363
36	None	2	356
36	None	20	360
50	None	2	366
27	Yes	2	370
27	Yes	13	360
27	Yes	20	355
27	Yes	36	347
27	Yes	50	347
50	Yes	2	344
50	Yes	7	335
50	Yes	13	332
50	Yes	20	332
50	Yes	36	336

[a]Zero at 62.1 nsec, pole at 6.2 nsec.

Table 2 Summary of Candidate High Sensitivity Fission Counter Designs

Fission Counter	Area (A)	Spacing (S)	Cap. (C) (A/S)	Collect. Time (T_c)	Charge/Pulse ($\bar{Q}$) PS	Gas Press. (P)	Voltage (V) S^2P/T_c	Drift Vel. (v_d) V/PS	Opt. Filt. τ (nsec)	N/$\sqrt{}$
HT-1	1	1	1	1	1	1	1	1	40	1
~~HT-2 ($Ar-CO_2$)~~										
HS-1	10	1	10	1	1	1	1	1	120	3.28
HS-2	10	2	5	1	1	1/2	2	2	60	2.14
HS-3	10	4	2.5	1	1	1/4	4	4	30	1.52
HS-4	10	2	5	1/2	1/2	1/4	2	4	30	1.30
HS-5	10	4	2.5	2	2	1/2	4	2	60	1.81
HS-6	10	2	5	2	2	1	2	1	50	1.51
HS-7	10	2	5	3	3	3/4	2	2/3	50	1.37
HS-8	10	2	5	4	4	2	2	1/2	50	1.30
HS-9	10	4	2.5	3	3	3/4	4	4/3	40	1.19
HS-10	10	4	2.5	4	4	1	4	1	40	1.14
HS-11	10	4	2.5	5	5	5/4	4	4/5	40	1.03
HS-12	10	4	2.5	6	6	3/2	4	2/3	40	1.02
HS-13 (Ar_7CO_2)	10	4	2.5	4	4	1	1.2	1	40	1.04